Jurnal Teknologi

Abstract

The Effect of Velocity in High Swirling Flow in Unconfined Burner

Norwazan A. R.[a,b*], Mohammad Nazri Mohd. Jaafar[b]

[a]*Faculty of Engineering, Universiti Pertahanan Nasional Malaysia, Kem Sg. Besi, 57000, Kuala Lumpur, Malaysia*
[b]*Department of Aeronautics & Automotive, Faculty of Mechanical Engineering, Universiti Teknologi Malaysia, 81310 UTM Johor Bahru, Johor, Malaysia*

*Corresponding author: norwazan@upnm.edu.my

Article history

Received :1 January 2014
Received in revised form :
15 February 2014
Accepted :18 March 2014

Graphical abstract

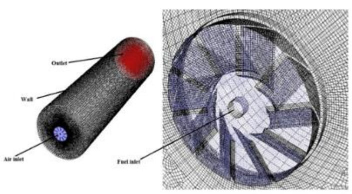

Abstract

This paper presents a numerical simulation of swirling turbulent flows in combustion chamber of unconfined burner. Isothermal flows with three different swirl numbers using axial swirler are used to demonstrate the effect of flow in axial velocity and tangential velocity on the center recirculation zone. The significance of center recirculation zone is to ensure a good mixing of air and fuel in order to get a better combustion. The inlet velocity, U_0 is 30 m/s entering into the burner through the axial swirler that is represents a high Reynolds number. A numerical study of non-reacting flow in the burner region is performed using ANSYS *Fluent*. The Reynolds–Averaged Navier–Stokes (RANS) standard *k-ε* turbulence approach method was applied with the eddy dissipation model. The paper focuses the flow field behind the axial swirler downstream that determined by transverse flow field at different on radial distances. The results of axial and tangential velocity were normalized with the inlet velocity. The velocity profiles are different after undergoing the different swirler up to the burner exit. However, the results of velocity profile showed that the high S_N gives a better swirling flow patterns.

Keywords: Burner; swirling flow; axial velocity; tangential velocity; standard *k-ε*

1.0 INTRODUCTION

Burner is widely used in most combustion industrial. In this burner, swirler is associated to merge and ensure the two streams of air and fuel have a good mixing. Swirlers are used as flame holders to control the mixture speed depending on the flame speed [1]. In addition, generating a swirling flow inside burners enhances the mixing of the different constituents of the mixture permitting, thus, a better control of the combustion process in terms of flame quality and pollutants emission.

Turbulent swirling flow in the burner plays an important role in controlling the combustion processes and performances. Swirling flows have been investigated extensively that used in all kinds of practical combustion systems including gas turbine combustor of aero-engine and industrial, swirl burner, furnaces, cyclone combustor and others [2, 3]. Consequently, the flame structure and stability in combustion is extremely dependent on the aerodynamics and mixing characteristics of fuel and oxidizer in their mixing region [3-6]. A swirling flow is the cause of an impartation of a tangential component by usage of swirler positioned within the burner [7]. The appropriate of swirl produces a large adverse pressure gradient in the direction of flow, which promotes the reverse flows. Thus, the formation of a flow pattern provides an aerodynamic blockage and reduced velocities necessary to stabilize the flame.

The prediction of the swirling flow characteristics in the combustor can be done using numerical simulation in order to optimize the design. A numerical study on the application of computational fluid dynamics (CFD) is a great potential in order to investigate isothermal and combustion process. Turbulence models that are great practical importance are three-dimensional and time-dependent. Computational methods of solving the differential equations of fluid dynamics are well advanced [8]. Turbulent behavior of inertial systems at every time in the space continuum seems to appear similar characteristics such as vortex structures and structural inhomogeneties. Turbulent is the state of fluid processing a non-regular or irregular motion such that velocity at any point may vary both in magnitude and direction with time. Turbulent motion is accompanied by the formulation of eddies and the rapid interchange of momentum in the fluid. Turbulence sets up greater stresses throughout the fluid and causes more irreversibility and losses. Turbulence is characterized by high levels of momentum, heat and mass transport due to turbulent diffusivity.

Mathur and Maccallum studied various angles of axial swirler. The flows showed that axial swirler of 60° vane angle has greater central recirculation vortex not only extended upstream to the hub of swirler but slightly blocked the annular flow area at the exit swirler. Thus, the axial swirler of 45° vane angle showed that central recirculation zone was firmly established. Matsubayashi examined the effect of swirler on swirling annular flow at several different vane angles, number of vanes and different hub diameters. The results showed that the reduction of hub diameter and number of vanes decreased the pressure drop while keeping high separator performances. But the reduction of vane angle deteriorates the separation performances liquid flow.

A recirculation zone is created downstream of the swirler in the center of flow. This is will effects primarily promoting fuel and air mixing and assisting the control of combustion temperature in the combustion zone. Therefore, the mixture provides the ignition energy for the fuel to ignite and stabilize the flame [9]. In non-premixed condition, fuel is injected in the shear region formed near the zero streamline boundary and recirculation region which provides the low velocity region for flame stabilization with the evolution of high temperatures from the flame. For flames operating in diffusion mode, the reaction zone is stabilized to result in large temperature gradients and hot-spot regions in the entire combustion chamber that result in high NO_x levels from the combustion of fuels [10].

The swirl intensity is generally characterized by the swirl number, defined as the ratio of the axial flux of azimuthal momentum to the axial flux of axial momentum [4, 7, 9, 11-13]. The swirl number is a measure of the strength of the swirling flow [14] as a main parameters used to characterize swirling flow [15]. Generally, the swirl number above 0.6 is indicated as a strongly swirling flow [16]. The swirl number is defined as:

$$S = \frac{G_\theta}{G_x R} \tag{3}$$

where,

$$G_\theta = \int_0^R \rho (Wr)\, u 2\pi r\, dr \tag{4}$$

and

$$G_x = \int_0^R \rho U^2 2\pi r \;\; dr \tag{5}$$

where U,W and ρ are the axial velocity, tangential velocity and density respectively. For axial swirler, the swirl number is related to the swirl angle, θ, inner r_i and outer radius r_0 as given by Beer which the swirl number was proportional to tan ϕ :

$$S_N = \frac{2}{3}\left[\frac{1 - \left(\frac{r_i}{r_0}\right)^3}{1 - \left(\frac{r_i}{r_0}\right)^2}\right] \tan\theta \tag{6}$$

Steady-state, incompressible, turbulent flows are governed by the Reynolds-averaged continuity and Navier-Stokes equations. The conservation form of these equations can be written as

Continuity:

$$\frac{\partial U}{\partial z} + \frac{1}{r}\frac{\partial}{\partial r}(rV) = 0 \tag{7}$$

Axial Momentum:

$$U\frac{\partial U}{\partial z} + V\frac{\partial U}{\partial r} = -\frac{1}{\rho}\frac{\partial P}{\partial z} + v\left(\frac{\partial^2 U}{\partial z^2} + \frac{1}{r}\left(r\frac{\partial U}{\partial r}\right)\right) - \frac{\partial}{\partial z}\langle u^2\rangle - \frac{\partial}{\partial r}\langle uv\rangle - \frac{\langle uv\rangle}{r} \tag{8}$$

Standard k-ε model the turbulent viscosity is computed by the combination of the turbulence kinetic energy, k and its dissipation rate, ε as follows

$$\mu_t = \rho C\mu \frac{k^2}{\varepsilon} \tag{9}$$

The two differential equations are used to describe the turbulence kinetic energy, k and dissipation rate of turbulence, ε in Equations (10) and (11), respectively [2, 8, 9, 17, 18]

$$\rho\frac{Dk}{Dt} = \frac{\partial}{\partial x_i}\left[\left(\mu + \frac{\mu_t}{\sigma_k}\right)\frac{\partial k}{\partial x_j}\right] + P - \rho\varepsilon \tag{10}$$

and

$$\rho\frac{D\varepsilon}{Dt} = \frac{\partial}{\partial x_j}\left[\left(\mu + \frac{\mu_t}{\sigma_\varepsilon}\right)\frac{\partial k}{\partial x_i}\right] + C_{1\varepsilon}\frac{\varepsilon}{k}P - C_{2\varepsilon}\rho\frac{\varepsilon^2}{k} \tag{11}$$

P represents the production of turbulence kinetic energy. The σ_k, σ_ε, $C_{1\varepsilon}$, $C_{2\varepsilon}$ and C_μ are model constants.

This paper investigates the isothermal flow to define the center recirculation zone that provide better mixing and combustion process. The axial swirler is adopted inside a burner and varied with different swirl number. The studies are presented using transverse flow field in different radial distance after flow entering air swirler downstream towards end of outlet burner.

2.0 METHODOLOGY

The Computational Fluid Dynamics (CFD) computer codes can be used as a numerical analysis to solve the governing equations. In CFD, the fluid flow can be predicted through arbitrary geometries that gives solution of flow speed, pressures, flow pattern etc. Initially, the Computer Aided Design (CAD) modeling was created using *AutoCAD 2012* software in three-dimensional (3D) according to the actual laboratory scale of liquid fuel burner. In the present study, the numerical simulation of swirling flow, issuing from the inlet of a burner, using standard k-ε turbulence models is considered. The 3D CAD modeling was assembled and exported to produce meshing and set-up the boundary conditions. The meshing was composed primarily of tetrahedral mesh elements including hexahedral, pyramidal and wedge with various sizes. 3D Reynolds-Averaged Navier Stokes (RANS) computations modeling of the entire section including swirl generation system and burner have been performed using commercial CFD-software namely ANSYS *Fluent*. Fluent computer code uses a finite-volume procedure to solve the RANS equations of fluid flow in primitive variables such as axial velocity, radial velocity and tangential velocity.

This study was focused on the cold flow model whereas is widely used for turbulence modeling and adopted for non-premixed combustion modeling. A 3D computational grid of 1.5 million cells was employed for the standard k-ε model simulation in order to simulate the isothermal flow in unconfined burner. The model constants for the standard k–ε model are C_μ = 0.09, $C_{1\varepsilon}$ =1.44, $C_{2\varepsilon}$ =1.92, and wall Prandtl number =1. The First Order Upwind Scheme was set for spatial resolution. The all RANS model were discretized using Quadratic Upstream Interpolation for Convection Kinetics (QUICK) and the SIMPLE algorithm was used.

At the front of burner, the air and fuel inlet and swirler are located with the element mesh were built in fine grids as shown in Figure 1. The burner with axial swirler has an outer diameter of 280 mm and the swirler diameter is 73 mm. The length of burner is 1000 mm as shown in Figure 2. The air inlet velocity is fixed at 30 m/s for all different swirler number to define the center recirculation zone. The transverse flow field data were measured at different location of burner length at *z*-planes as shown in Figure 2. In this study, 3 different swirl numbers are studied including $S_N = 0.436$, $S_N = 0.630$ and $S_N = 0.895$.

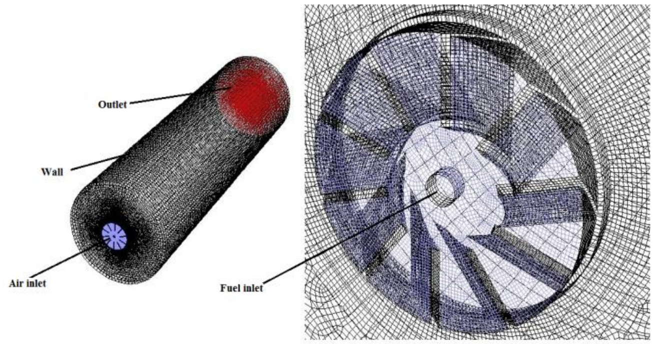

Figure 1 The mesh modeling of unconfined burner including the axial swirler

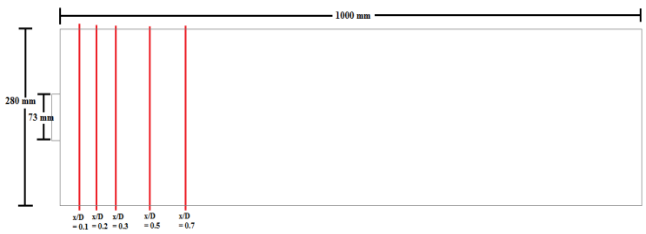

Figure 2 The transverse flow field in *z*-plane

3.0 RESULTS AND DISCUSSION

The velocity magnitude along the combustor is measured using experimental and numerical method. Figure 3 shows good agreement results between both methods in axial direction along the combustion chamber of burner. The experiment data is measured in axial distance at 10 different locations at the center core of flow. This comparison data used the same parameter that was investigated such as same input velocity at 30 m/s and 50 degree of swirl vane angles. They showed that the numerical simulation result has similar trend of velocity magnitude with the experimental data.

Swirling jet flow is the results of impartation of axial velocity that produced by swirl generator. The large reverse flow zone that induced by the vanes of swirler in axial direction is identified by negative axial velocity in isothermal condition known as center recirculation zone. There are also other recirculation zones at the corner of the chamber namely corner recirculation zone. Comparison of the flow patterns results at air velocity inlet is 30 m/s shows similarity between three various swirl number which represented different swirl vane angles. These results presented are the axial and tangential velocity in radial distance where it shows the strength of swirl flow that influenced by axial and tangential velocities components [19].

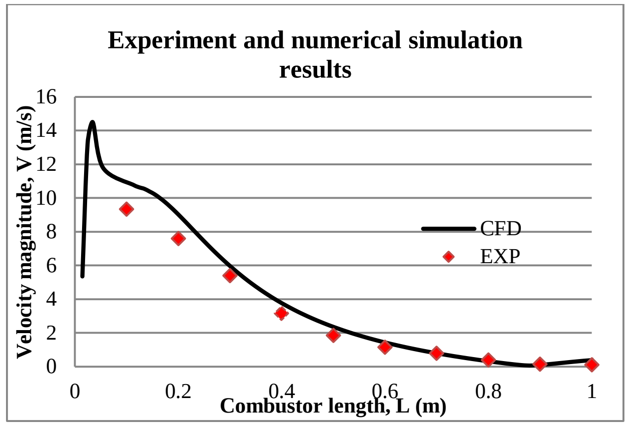

Figure 3 Velocity magnitude profile along combustor

Figure 4 shows the reverse velocity distribution contour, termed as central recirculation zone in the mid plane for each case of S_N of 30˚, 40˚ and 50˚ vane angle respectively. The flow downstream of 50˚ swirler has a maximum reverse velocity of 12.34 m/s. Thus the maximum reverse velocity magnitudes of 40˚ and 30˚ vane angle are found as 10.84 m/s and 7.11 m/s. These contours are displayed by plotting the negative axial velocities with ranges from 0 to maximum negative axial velocity flow within the entire recirculation zone. As seen in Figure 4, the recirculation zone of 50˚ is more width and longer. It shows that the central recirculation zone has a largest width and length by increases the S_N. As reported [19], the effect of various axial swirler in square chamber also illustrated that the length and width of recirculation zone increased with increase in the vane angle.

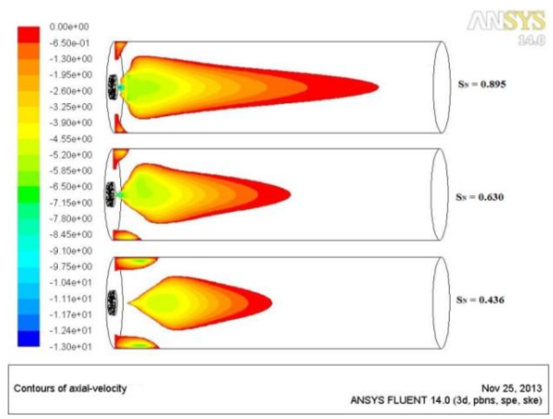

Figure 4 The contour of reverse velocity flow

Axial Velocity Profiles

Principle importance of axial velocity profiles is illustrated by jet boundary, degree of expansion and region of high velocity gradient [13]. It is also defined by the boundaries of the forward- and reverse-flow zones. Generally, the zone behind swirler placed in strong axial stream and their formation of a downstream known as recirculation zone depends on the S_N and Reynold's number [20]. The axial velocity profiles of each swirl number compared in Figure 4 shows a good agreement at downstream of swirler. In the upstream condition, the flow-entering the burner with different swirl number has a different pattern flow stream in radial distance.

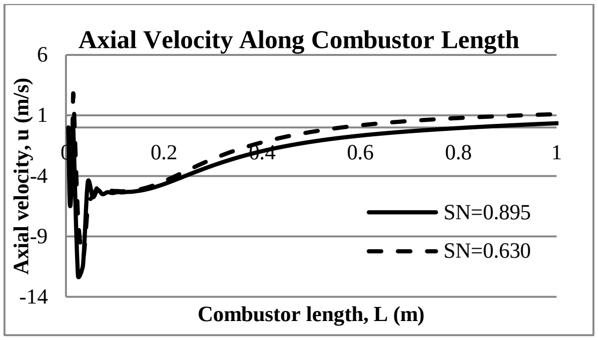

Figure 5 Comparison of axial velocity along combustor length

In Figure 5, the reverse velocity has been plotted due to the axial direction along the combustion chamber downstream of swirler exit. From these result, it shows that the reverse velocity has a highest value by increasing the S_N. Then, the reverse velocity keep decreasing after z = 0.015 mm to positive velocity towards the outlet.

Figure 6 showed the contour of axial velocity of each swirl number and at different of x/D plane. The contour is related to the axial velocity graphs along radial distance. A low S_N has narrow and lowest reverse velocity at early flow entering combustion chamber throughout the axial swirler. But the swirling flow with high S_N is wider and has highest reverse velocity. It looks more stable and produced better mixing between air and fuel in combustion process.

The velocity profiles are normalized with respect to the inlet velocity, U_0 of 30 m/s as shown in Figure 7. The reverse velocity profiles also observed that the high swirl number (S = 0.895) has a highest reverse velocity at the first transverse plane of x/D = 0.1 that indicated effectively the axial velocity distribution leaving the swirler. But the low swirl number (S = 0.436) has a lowest reverse velocity or the reverse flow occurred at the center of flow after entering the swirler. The reverse velocity appeared in two negative-velocity regions indicating existence of the center recirculation zone and corner recirculation zone [18]. Zhuowei found that the peak of reverse velocity for standard k-e model is close to the central region for low and high swirl equal to 19 m/s and 23 m/s respectively [21]. But this peak of reverse velocity for high swirl occurred at r = 0.04 mm and for low swirl, at r = 0.02mm. It shows that by increasing the swirl number, the maximum reverse velocity occurred far from center region of burner.

Xia had studied the comparison of swirling flow in annular cylindrical tube using different k-e turbulence models [18]. The result of axial velocity indicates the existence of central recirculation zone and corner recirculation zone at x/D = 0.2 plane. The reverse flows of each case started changed from x/D = 0.2 towards downstream. The axial velocity profiles are showed the forward flow to be mainly in the outer part of jet flow with peak velocities increasing with swirl number. The low swirl number started to flatten in radial distance slowly at x/D = 0.3. Thus, the trends were continued in the similar flow pattern concurrently by increasing swirl number along x/D ratio. In this observation, it shows that the high swirl number gives an improvement on swirling flow and thus provides a good mixing of air fuel in combustion process later.

Tangential Velocity Profiles

Figure 8 illustrates the tangential velocity profiles for each case of swirl number at different x/D ratio. Highest swirl number provides a highest peak of tangential velocity that occurred near to the center of burner. In early stage, as low as swirl number, the tangential velocity was moved forward in axial direction is lowest than the others but the expands in radial distance. In this isothermal case, the tangential velocities in Figure 8 are shows that the velocities diminish as the flow expands along the wall for each plane and case. These flow fields in tangential velocity are well predicted near the inlet of axial swirler in center region.

Raj found the numerical results and the experimental results have a good agreement for 15˚, 30˚, 45˚ and 60˚ angles and the trend of swirling flow are well predicted. For higher S_N, the maximum tangential velocity values are far from the center flow in core region. However, the findings of tangential velocity and flow patterns by Raj are similar and behave in same condition compared with this study [19]. As expected, the tangential velocity values are succeeded in maximum at the x/D plane at nearly to the swirler and start decreasing towards downstream.

As shown in Figure 6, there are also can be seen that the position of maximum tangential velocity moves towards the wall [18]. For higher S_N, this tangential velocity is highly achieved near to the wall. Observation from Zhuowei, it found that the tangential velocity value exhibits the forced-vortex characterized by increased the tangential velocity in central region while the free-vortex characterized by decreased the tangential velocity when approaching the wall [21]. The similar finding in this results, the tangential velocity presented that is increasing and moves forward to the walls in high S_N. For low S_N, the tangential velocity is keep reducing in the center region as far as from swirler. These results show that the potential of the axial swirler especially in high S_N to stabilize the swirling flow and get better mixing of air and fuel to use in unconfined burner. It is also shows that the standard k-e model is able to predict the swirl behavior even for a weak swirl but it is still reasonable.

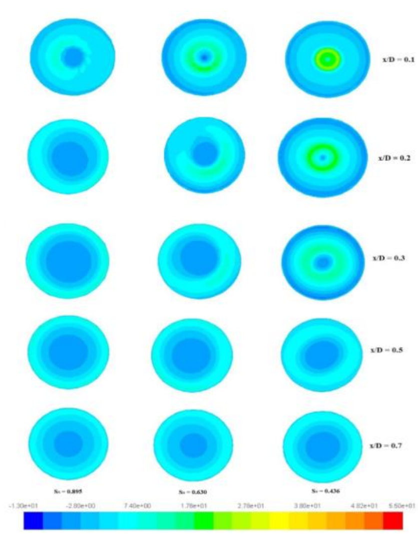

Figure 6 Contour of axial velocity of various swirl number and x/D at z-plane

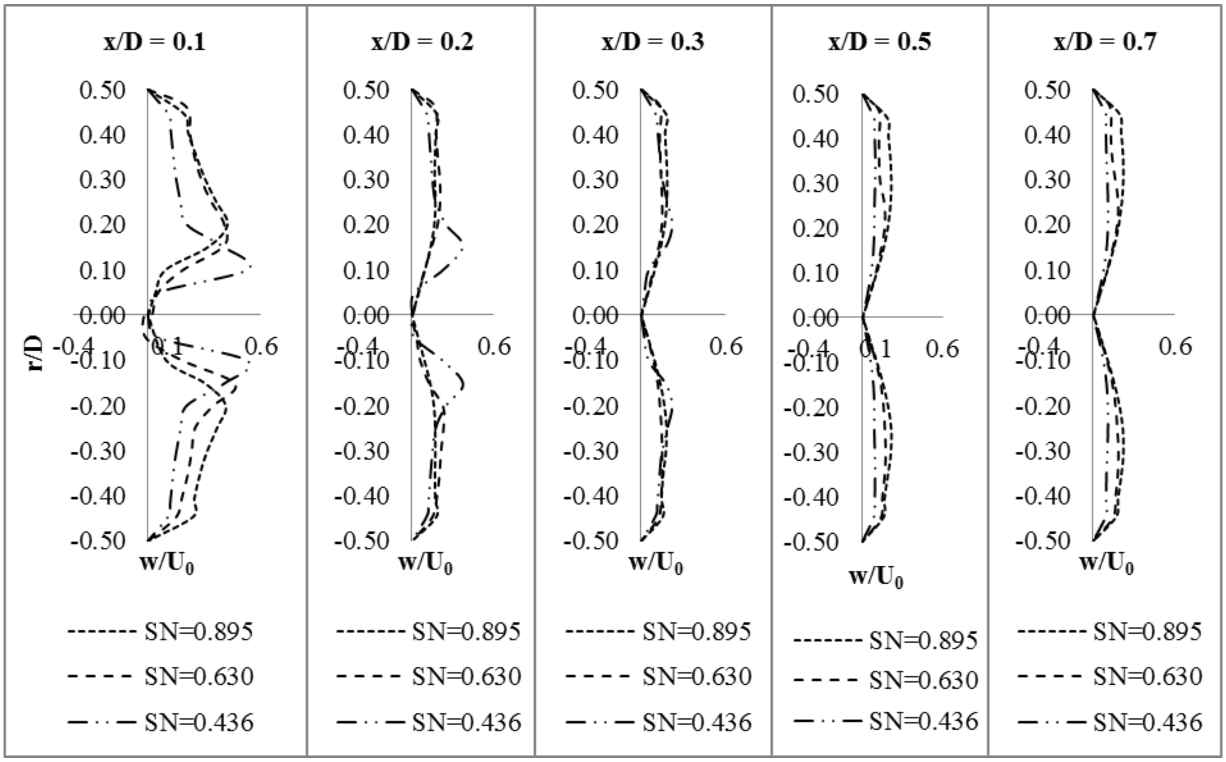

Figure 7 Axial velocity profiles

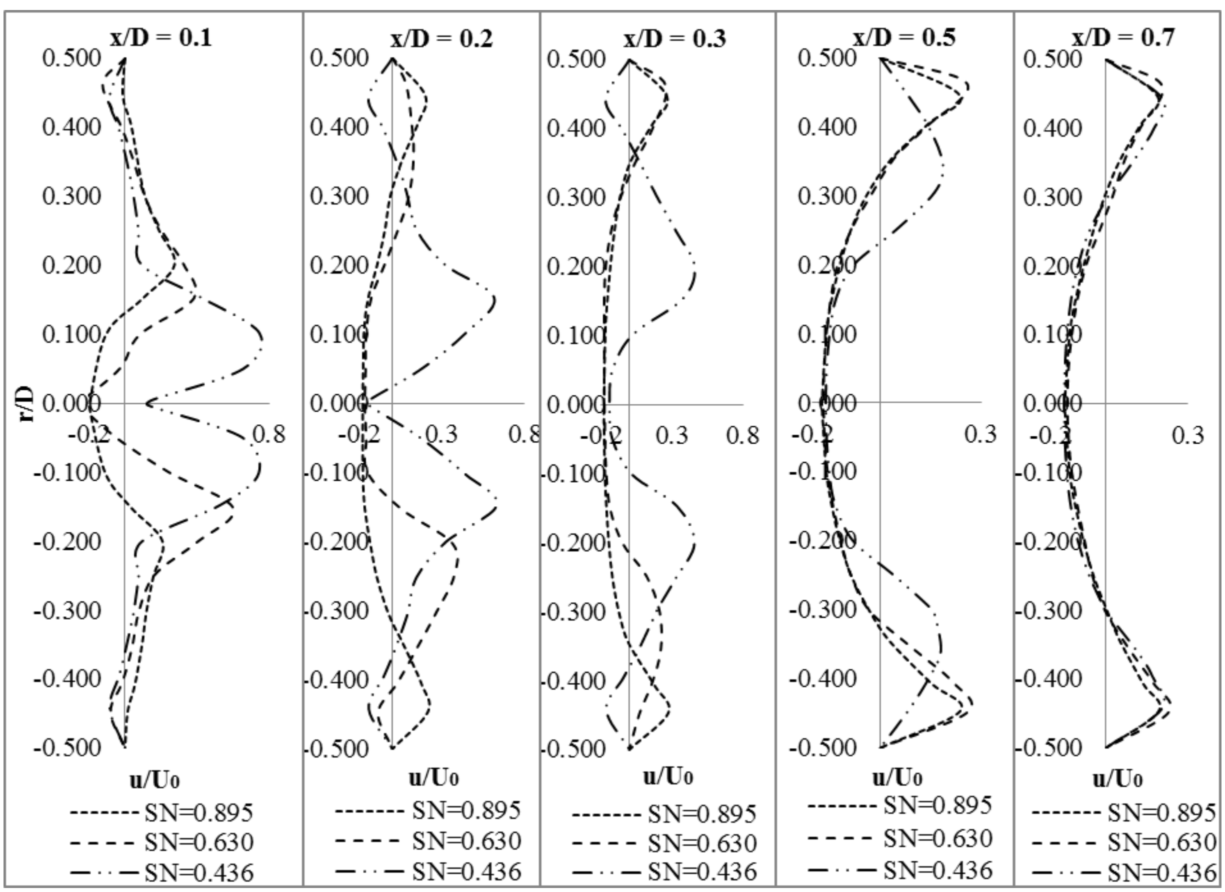

Figure 8 Tangential velocity profiles

■4.0 CONCLUSION

The standard *k*-*ε* turbulence approach method was used in this study to evaluate the axial swirler adopted inside an unconfined burner are well compared. The simulation is defined by axial and tangential velocity with the various swirl numbers. This study also was investigated to determine a better center recirculation zone in order to get better mixing with a suitable vane angle of axial swirler using standard *k*-*ε* turbulence model are still reasonable. The graph axial velocity and tangential velocity are shows that the obvious different are occurred at the early *z*-planes after the flow entering the burner throughout the axial swirler. After x/D = 0.3 plane, the both velocities are shows the graph pattern are starting changes in similar pattern for all swirl number. It seen that the swirling is affected at the early in swirler downstream that given a larger effect by S_N. It can be concluded that with high S_N is produced a better mixing and good swirling flow with attached in unconfined burner.

Acknowledgements

The authors would like to thankful to Ministry of Science, Technology and Innovation (MOSTI) for their funding under Sciencefund Grant 4S046 as well as UTM for their supports.

References

[1] Mohd Jaafar, M. N., Jusoff, K., Osman, M. S., and Ishak, M. S. A. 2011. Combustor Aerodynamics Using Radial Swirler. *International Journal of Physics Sciences*. 6(13): 3091–3098.

[2] Ridluan, A., Eiamsa-ard, S., and Promvonge, P. 2007. Numerical Simulation of 3D Turbulent Isothermal Flow in a Vortex Combustor. *International Communication in Heat and Mass Transfer*. 34: 860–869.

[3] Litvinov, I. V., Shtork, S. I., Kuibin, P. A., Alekseenko, S. V., and Hanjalic, K. 2013. Experimental Study and Analytical Reconstruction of Processing Vortex in a Tangential Swirler. *International Journal of Heat and Fluid Flow*. 42: 251–264.

[4] Syred, N., and Beer, J. M. 1974. Combustion in Swirling Flows: A Review. *Combustion and Flame*. 23: 143–201.

[5] Sloan, D. G., Smith, P. J., and Smoot, L. D. 1986. Modeling of Swirl in Turbulent Flow Systems. *Prog. Energy Combustion Science*. 12: 163–250.

[6] Eldrainy, Y. A., Mohd Jaafar, M. N., and Mat Lazim, T. 2008. Numerical Investigation of the Flow Inside Primary Zone of Tubular Combustor Model. *Jurnal Mekanikal*. 26: 162–176.

[7] Yegian, D. T., and Cheng, R. K. 1998. Development of a Vane-swirler for Use in a Low No_x Weak-Swirl Burner. *Combust. Sci. Technol.* 139(1–6): 207–227.

[8] Launder, B. E., and Spalding, D. B. 1974. The Numerical Computation of Turbulent Flows. *Computer Methods in Applied Mechanics and Engineering*. 3: 269–289.

[9] Eldrainy, Y. A., Saqr, K. M. Aly, H. S., and Mohd Jaafar, M. N. 2009. CFD Insight of the Flow Dynamics in a Novel Swirler for Gas Turbine Combustors. *International Communications in Heat and Mass Transfer*. 36: 936–941.

[10] Khalil, A. E. E. and Gupta, A. K. 2011. Distributed Swirl Combustion for Gas Turbine Application. *Applied Energy*. 88: 4898–4907.

[11] Orbay, R. C., Nogenmyr, K. J., Klingmann, J., and Bai, X. S. 2013. Swirling Turbulent Flows in a Combustion Chamber with and Without Heat Release. *Fuel*. 104: 133–146.

[12] Pollard, A., Ozem, H. L. M., and Grandmaison, E. W. 2005. Turbulent, Swirling Flow Over an Asymmetric Constant Radius Surface. *Experimental Thermal and Fluid Science*. 29: 493–509.

[13] Beltagui, S. A., Kenbar, A. M. A., and Maccallum, N. R. L. 1993. Comparison of Measured Isothermal and Combusting Confined Swirling Flows: Peripheral Fuel Injection. *Experimental Thermal and Fluid Science*. 6: 147–156.

[14] Murphy, S., Delfos, R., Pourquie, M. J. B. M., Olujic, Z., Jansens, P. J., and Nieuwstadt, F. T. M. 2007. Prediction of Strongly Swirling Flow within an Axial Hydrocyclone Using Two Commercial CFD Codes. *Chemical Engineering Science*. 62: 1619–1635.

[15] Syred, N., Abdulsada, M., Griffiths, A., Doherty, T.O., and Bowen. 2012. The Effect of Hydrogen Containing Fuel Blends Upon Flashback in Swirl Burners. *Applied Energy*. 89: 106–110.

[16] Grech, N., Koupper, C., Zachos, P.K., Pachidis, V., and Singh, R. 2012. Consideration on the Numerical Modeling and Performance of Axial Swirlers Under Relight Conditions. *Journal of Engineering for Gas Turbines and Power*.

[17] Datta, A., and Som, S. K. 1999. Combustion and Emission Characteristics in a Gas Turbine Combustor at Different Pressure and Swirl Conditions. *Applied Thermal Engineering*. 19: 949–967.

[18] Xia, J. L., Yadigaroglu, G., Liu, Y.S., Schmidli, J., and Smith, B. L. 1998. Numerical and Experimental Study of Swirling Flow in a Model. *Int. Journal Heat Mass Transfer*. 41(11): 1485–1497.

[19] Raj, R. T. K., and Ganesan, V. 2008. Study on the Effect of Various Parameters on Flow Development Behind Vane Swirlers. *International Journal of Thermal Sciences*. 47: 1204–1225.

[20] Al-Abdeli, Y. M., and Masri, A. R. 2003. Recirculation and Flowfield Regimes of Unconfined Non-reacting Swirling Flows. *Experimental Thermal and Fluid Scienc*. 27: 655–665.

[21] Zhuowei, L., Kharoua, N., Redjem, H., and Khezzar, L. 2012. RANS and LES Simulation of a Swirling Flow in a Combustion Chamber With Different Swirl Intensities. *Proceeding of CHT-12, ICHMT International Symposium on Advances in Computational Heat Transfer*.